Journal of Radiotherapy in Practice

cambridge.org/jrp

Estimation of monitor unit through analytical method for dynamic IMRT using control points as an effective parameter

M. Athiyaman[1], A. Hemalatha[1], Arun Chougule[2], Mary Joan[2] and HS Kumar[1]

[1]Radiological Physics, Sardar Patel Medical College, Bikaner, Rajasthan, India 334003 and [2]Radiological Physics SMS Medical College and Hospital, Jaipur, Rajasthan, India 302004

Original Article

Cite this article: Athiyaman M, Hemalatha A, Chougule A, Joan M, and Kumar HS. (2022) Estimation of monitor unit through analytical method for dynamic IMRT using control points as an effective parameter. *Journal of Radiotherapy in Practice* **21**: 343–350. doi: 10.1017/S1460396921000017

Received: 1 November 2020
Revised: 19 December 2020
Accepted: 31 December 2020
First published online: 2 March 2021

Key words:
computer-assisted radiotherapy; radiotherapy dosage; radiotherapy planning

Author for correspondence:
M. Athiyaman, Radiological Physics, Sardar Patel Medical College, Bikaner, Rajasthan, India 334003. E-mail: athiyaman.bikaner@gmail.com

Abstract

Introduction: The control points (CP) play a significant role in the delivery of segmented based Intensity-Modulated Radiation Therapy (IMRT) delivery, particularly in dynamic mode. The number of segments is determined by control points and these segments will transfer from one to the other either during beam ON called dynamic delivery or during beam OFF called static delivery or step and shoot. This study was aimed at indirect estimation of the total monitor units (MU) to be delivered per field by exploiting the control points and also to find the MUs at any n^{th} segment.

Materials and methods: This study was performed in the Eclipse treatment planning software version 13.8.0. The details of control points, metre set weight per segment, leaf positions for each segment, field size, etc. were taken into consideration.

Results: TPS calculated MU value and analytically estimated MU value were compared and the percentage of difference was estimated. The overall mean percentage of deviation was 1·03% between the TPS calculated method and the analytical method. The paired sample *t*-test was performed and, *p*-value <0·05, no significant difference was found. The analytical relationship determined to estimate the total number of MU delivered for any n^{th} control point was also evaluated.

Conclusion: The control points are a potential parameter in the conventional IMRT delivery. Through this study, we have addressed the indirect method to estimate the monitor units delivered per segment.

Introduction

Intensity-Modulated Radiation Therapy (IMRT) is a further refinement of the segmented beam technique in which each of the treatment fields is made up of many segments. IMRT optimally assigns non-uniform intensities (i.e., weights) to tiny subdivisions of beams, which have been called rays or 'beamlets'. The objective is to produce higher conformity than is achievable with conformal blocked fields. In IMRT each radiation beam is divided into many subfields.[1] The ability to optimally manipulate the intensities of individual rays within each beam permits greatly increased control over the radiation fluence, enabling the custom design of optimum dose distributions.[2] These improved dose distributions potentially may lead to improved tumour control and reduced normal tissue toxicity.[3–11]

In advanced delivery techniques, such as intensity-modulated radiotherapy (IMRT) and volumetric-modulated arc therapy, the multi-leaf collimators (MLCs) are employed to dynamically shape the beam during the delivery[12–16] to achieve highly conformal dose distributions.

By delivering typically five to seven beams with an individualised intensity profile, the dose is conformed to the volume and normal tissue and critical organs spared.[17] The individual treatment beams for IMRT can be delivered using MLCs in either dynamic or multiple-segment ('step and shoot') mode. The complexity of IMRT plans may originate from the design of inverse planning systems, typically using pixel-based or fluence-based optimisation. In general, this type of optimisation first divides a broad beam into many small beamlets (e.g., 1 cm × 1 cm), and then the intensities of these beamlets are adjusted according to the planning dose objectives to minimise the value of an objective function.[18] Finally, the optimised intensity patterns are decomposed into a series of deliverable MLC shapes (segments) each associated with a uniform dose. This decomposition step is referred to as leaf sequencing. The entire process is known as two-step optimisation.[19–21]

Among various issues related to verifying the treatment, a pressing problem is how to verify efficiently the calculation of monitor units (MU) from a commercial inverse planning system. An independent MU check is required for patients treated through complex techniques such as

CAMBRIDGE UNIVERSITY PRESS

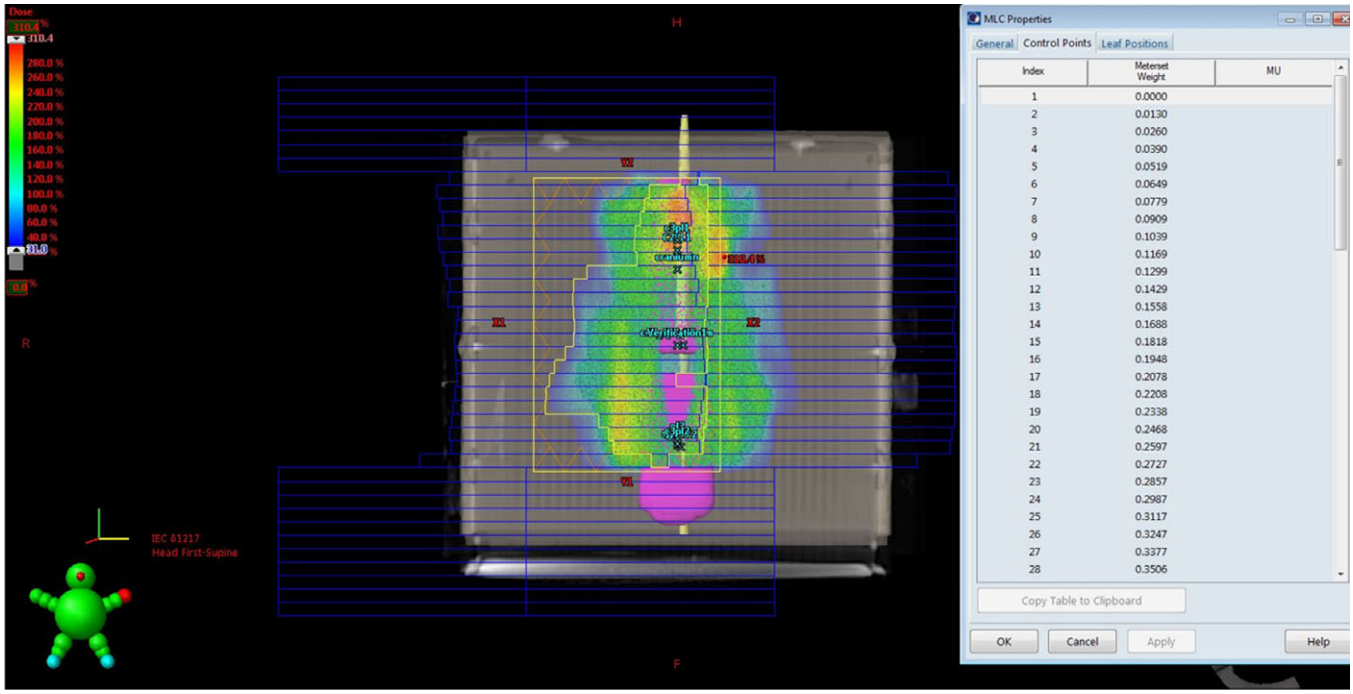

Figure 1. IMRT fluence delivered in phantom and respective control points.

IMRT, IGRT, etc.[22] It is standard practice in external beam radiotherapy (EBRT) to verify independently the calculation of MU before the start of patient treatment. For intensity-modulated radiotherapy, an independent calculation of MU becomes difficult due to the complex relationship between the MU and the beam-intensity modulation shape as well as the technique used to generate the intensity modulation.[23] Several authors experimented with methods to verify monitor unit checks through analytical calculations. The MU calculation for a multi-leaf collimated static field has been described in the literature.[24] A few attempts have been made to develop more efficient techniques for the verification of dynamic delivery. Boyer et al. have investigated some theoretical aspects of the MU calculation for an intensity-modulated field.[25]

The control points (CP) play a significant role in the delivery of segmented based IMRT delivery, particularly in dynamic mode.[26] The dynamic delivery sequence is approximated with multiple segments or subfields that deliver a fixed number of monitor units for specific leaf positions, collimator angle and gantry angle called as control points. These segments will transfer from one to the other either during beam ON called as dynamic delivery or during beam OFF called as static delivery or step and shoot. A dynamic delivery IMRT field file will contain several control points at a marked fraction of the delivered monitor units, which are specified as MLC shapes. Deliverable fluence fidelity is proportional to the number of control points defined.

The present study is aimed to exploit the features of control points and estimate an indirect approach for estimating the monitor units per segment in a dynamic IMRT delivery.

Materials and Methods

This study was performed in the Eclipse treatment planning system (TPS) version 13.8.0. (Make: Varian Medical Systems, Palo Alto, USA). The treatment plans of patients who received Intensity-modulated Radiotherapy were selected for this study. A total of 30 patient's plans were randomly selected with 10 each for the head and neck region, cranium and cervix for monitor unit verification calculation (MUVC). The IMRT plans were optimised by the Photon Optimizer algorithm and the calculated fluence was delivered through MLC. The movements of MLCs were calculated by the leaf motion calculator. Dose calculation was performed by an Anisotropic and Analytical algorithm with a spatial resolution of 0·25 cm.

The Linear accelerator in which this study performed was Clinac 2300CD, (Make Varian Medical Systems, Palo Alto, USA) which can deliver dynamic and static IMRT with 40 pairs of MLC. The dynamic delivery was approached with more 'segments' or 'subfields' each will deliver a fixed number of monitor units. These segments had different aperture shape according to the fluence required to deliver in that particular phase. The calculated fluence was delivered with the gantry and collimators fixed. The segments were delivered dynamically, that is, the transition from one segment to the other while beam ON and the same were converted into control points to execute the IMRT delivery in the linear accelerator machine. Each control point defined had specific leaf positions of bank A and bank B that form the aperture by which the MUs were delivered. The control points were assigned metre set weight according to the field size and dose to be delivered through that field. The first control point always had a value of zero with variable parameters gantry, collimator angle, and field size of the first segment. The second control points have the cumulative MU of the first segment but with the aperture of the first segment. The transition from the second to the third segment delivered the MU of the first segment. Thus the complete segmented based dynamic IMRT was delivered.

In our study, we attempted to estimate the total monitor units to be delivered per field by exploiting the control points of a specific field. This would give an indirect method to estimate the MU per

https://doi.org/10.1017/S1460396921000017 Published online by Cambridge University Press

field and the total MU for the complete treatment can be estimated. The MLC properties will have the details of control points, metre set weight per segment, leaf positions for each segment, field size, etc. Additionally, it will provide the information of the total MU for the particular field at the end of the control point. The IMRT plans were transferred to the I'MatriXX phantom as similar to fluence verification for patient-specific QA, Figure 1.

(i) Estimation of monitor unit per segment:

The total MU calculated depends on the field area to be covered, dose prescribed at the depth of the patient, and the number of beams used in the plan. The control points also an important parameter for MU delivery. We derived a conceptual equation for estimating the MU delivered for each segment.

$$\mathbf{MU_{seg}} = \frac{\mathbf{MU_{cal}}}{\mathbf{\Sigma\ no\ of\ control\ points}} \quad (1)$$

where

$\mathbf{MU_{cal}}$ = Total MU calculated by the TPS
$\mathbf{MU_{seg}}$ = MU per segment
C.P = control points of the field

This equation depicts that the control point plays a vital role in the delivery of MU for the IMRT fields. The number of control points was taken from the MLC plan properties for each field. The calculated MU per segment from the above-mentioned formula was to estimate the total MU required to deliver the total MU for the field. The calculated total MU by the newly developed method was compared with the TPS calculated MU and comparisons were made between the two methods.

(ii) Estimation of MU delivered up to n^{th} control point:

The MU per segment was considered as a modulation factor that determines the MU for any control point. The total MU delivered up to n^{th} can be found at any of the in-between control points by summing up the metre weight up to the n^{th} control point.

$$\mathbf{MU_{c.p}} = \mathbf{MU_{seg}} \times \mathbf{\Sigma CP_i} \quad (2)$$

where

$\mathbf{MU_{C.P}}$ = Monitor unit delivered up to n^{th} control point
$\mathbf{MU_{seg}}$ = MU per segment
$\mathbf{\Sigma CP_i}$ = i^{th} control point

Through Equation (1) MU per segment was calculated and total MU for any field was estimated. The treatment plan of seven field techniques was taken for the study. Equal field weight was given for all the seven fields. The MU estimated through Equation (1) was compared with the TPS calculated MU and the comparison was made between the proposed analytical method and the TPS calculated method.

The total MU that would be delivered for any in-between segments can be estimated by building the relationship between the control point and the MU per segment. The relationship will be mostly of linear equations $y = ax + b$, where y = MU per segment, x = control point.

Table 1. Treatment sites have taken for MUVC verification

Sr. no.	Site	Treatment technique	No. of fields taken for MUVC
1	Head and Neck	Dynamic IMRT	10
2	Cranium	Dynamic IMRT	10
3	Cervix	Dynamic IMRT	10

Table 2. Fields have taken for finding relationships between the control point and monitor unit

Sr. no.	Field name	Total MU TPS	MU per Beamlet	Total control Points
1	AP	233	1·159	201
2	LAO	186	1·338	139
3	LL	147	0·7736	190
4	LPO	216	1·1016	203

$$\mathbf{MU\ for}\ n^{th}\ \mathbf{control\ point} = \mathbf{MU\ per\ segment} \times n^{th}\ \mathbf{control\ point} + \mathbf{intercept\ (zero\ control\ point)} \quad (3)$$

(iii) Verification by measurements:

The method of total MU estimation was verified by the dosimetry performed through the point dosimetry method and also with I'MatriXX detector array (Make: Scanditronix Wellhofer). The plans were transferred to the I'MatriXX scanned phantom and tissue-equivalent phantom in Eclipse TPS as a routine method of plan verification. All the fields were placed in gantry zero position and dose calculation was performed again. The procedure previously outlined for the estimation of total MU for each section were performed. Dose calculated plans were transferred through the record and verify mode to the control computer. The externally calculated MU were delivered through the service mode of this Linac to compare the dose delivered to the calculated dose by the TPS.

The MLC files were exported from the TPS and the same files were reproduced in the MLC shaper software. The shaper software was used to regenerate the MLC leaf positions for each segment. These reinforced MLC leaf positions were transferred to the control console of Linac. By doing so we had the independency of delivering the desired MU for any segments.

The calculated MU by the above-mentioned methods was delivered and the dose at the reference point was estimated. The usage of I'MatriXX helped not only for estimating the dose delivered at the isocenter but also the overall fluence in the plane estimation.

The dose estimated by the I'MatriXX system and the dose calculated by the TPS were both compared (Figure 3, Table 4)

(iv) Estimation of MU delivered up to n^{th} control point:

The fields identified for finding the linear relationship between MU per segment and control points are shown in Table 2.

https://doi.org/10.1017/S1460396921000017 Published online by Cambridge University Press

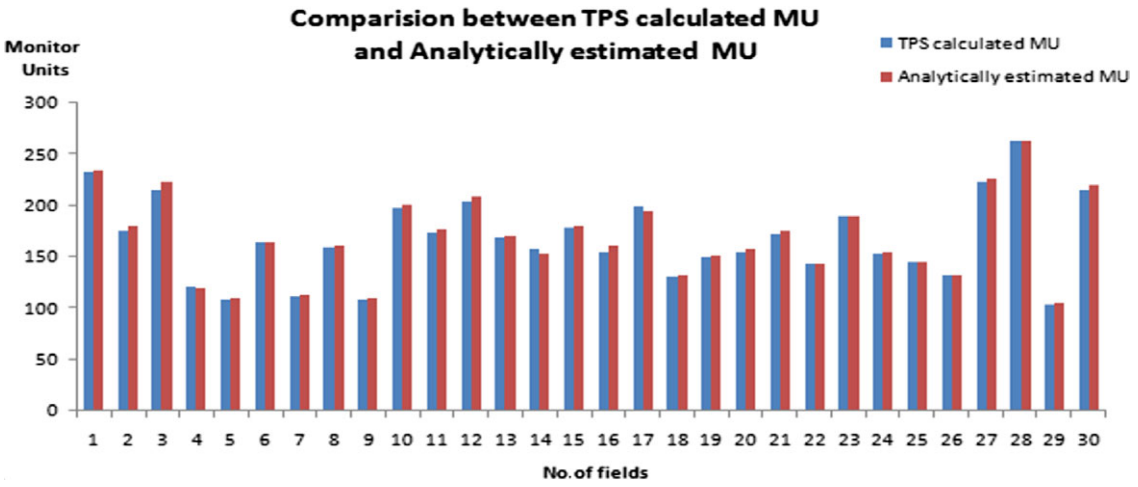

Figure 2. Comparison between TPS calculated MU and analytically estimated MU.

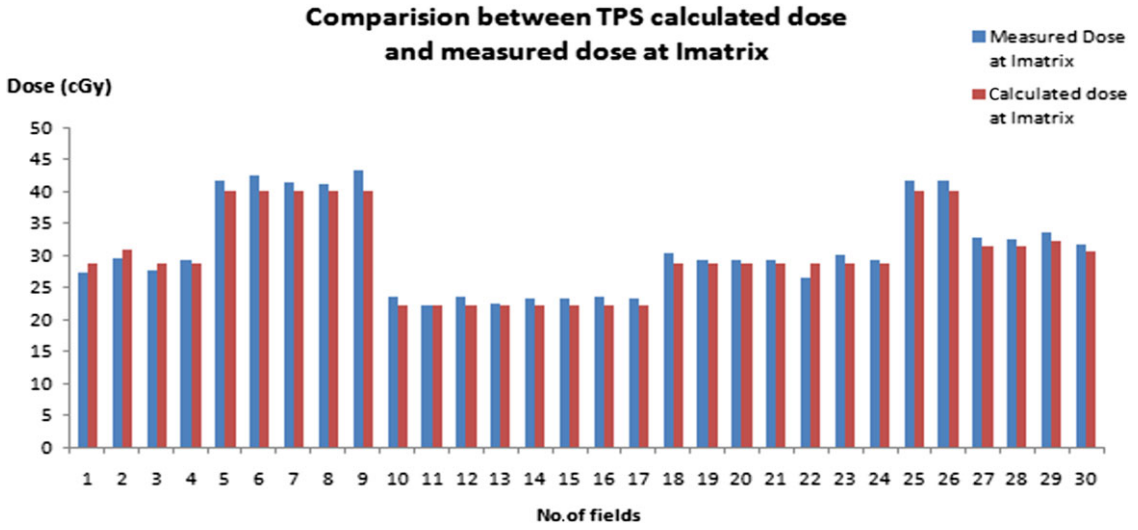

Figure 3. Comparison between TPS calculated dose and measured dose at I'MatriXX.

Results

A total of 30 cases were taken for evaluation from the head and neck region, cranium, and cervical cancers respectively as described in Table 1. As mentioned in the formula . . . .1 MU per segment was estimated from the inputs, total MU for the field, and the total number of control points. Through the analytical method, we estimated the total number of monitor units required with the help of the total number of control points and MU per segment.

A comparison was made between the TPS calculated MU value and analytically estimated MU. Fields namely anteroposterior (AP), left anterior oblique (LAO), left lateral (LL), and left posterior oblique (LPO) taken for evaluation Table 2. The comparison of these two methods of estimation is described in Figure 2 and Table 3.

The percentage of deviation between TPS calculated MU and analytically estimated MU was also determined. The mean percentage of deviation was 1·03 and p-value <0·05, Table 5. The overall mean percentage of deviation was 1·03% between the TPS calculated method and the analytical method. The paired sample t-test was performed and, p-value <0·05, no significant difference was found.

Discussion

The intensity modulation of radiation delivery has had a positive impact on the delivery of treatment using radiotherapy and has greatly expanded the opportunities of the specialty. IMRT being a potential and robust technique in delivering the desired fluence according to the tumour shape and size by reducing the dose to nearby normal structures. Even though IMRT can be delivered by various delivery methods it can be potentially delivered in a simplified way with the MLC. The most common IMRT delivery requires the use of moving MLCs to deliver the requested fluence pattern.[25] In dynamic IMRT, the required pattern of dose distributions is delivered through the small segments.[26,27]

https://doi.org/10.1017/S1460396921000017 Published online by Cambridge University Press

Table 3. Control point and comparison of MU between analytical method and TPS

Sr. no.	Field details	Dose per field (cGy)	No. of control points	TPS calculated MU	Analytically estimated MU	Percentage difference
1	**AP**	28·571	201	233	234·165	0·5
2	**LAO**	30·714	113	175	179·953	2·83
3	**LPO**	28·571	203	216	223·625	3·53
4	**RL**	28·571	122	122	119·902	−1·72
5	**RAO**	40	90	108	109·836	1·7
6	**LPO**	40	106	164	165·148	0·7
7	**AP**	40	107	111	112·832	1·65
8	**LAO**	40	99	159	160·558	0·98
9	**RAO**	40	90	108	109·836	1·7
10	**AP**	22·222	212	198·2	201·688	1·76
11	**LAO**	22·222	193	173·9	177·882	2·29
12	**LL**	22·222	197	204	208·978	2·44
13	**PA**	32·143	165	169	170·099	0·65
14	**PA**	22·222	167	158·4	153·426	−3·14
15	**RPO**	22·222	183	178·8	179·962	0·65
16	**RAO**	22·222	200	154·5	160·68	4
17	**RPO1**	22·222	212	200·1	195·138	−2·48
18	**LPO**	28·571	126	131·3	132·35	0·8
19	**LL**	28·571	99	150	151·47	0·98
20	**LAO**	28·571	124	155·2	157·807	1·68
21	**AP**	28·571	159	172·9	175·943	1·76
22	**RAO**	28·571	110	143·8	143·944	0·1
23	**LPO**	28·571	161	190	189·658	−0·18
24	**RPO**	28·571	129	153·1	154·049	0·62
25	**AP**	40	138	144·7	145·771	0·74
26	**LAO**	40	144	132	133·056	0·8
27	**AP**	31·429	159	223	226·925	1·76
28	**LAO**	31·429	239	263	263·999	0·38
29	**RL**	32·143	113	104	105·768	1·7
30	**AP**	30·429	182	216	220·147	1·92

The relationship between the MU and control points were studied for five cases as mentioned in Figures 4 and 5. The parameters namely the number of control points, TPS calculated MUs were taken for analytical MU estimation. The relationship between MU and control points has shown that the MUs have a highly linear relationship with the control points. The correlation co-efficient resulting in near to unity proves the fact. With this relationship, we can estimate the total number of MU delivered for any n^{th} control point. The MUs for any n^{th} control point can be estimated with the help of formula . . . (2). Through this study, an attempt was made to estimate the monitor units delivered per control points. We have explored the control point's functionality and the monitor unit per segment was estimated.

For complex head and neck cases, as many as 130–160 segments with 9 beam angles are needed.[28] Studies have been performed by various authors concerning an attempt to reduce the number of segments in IMRT delivery. The reduction of radiation efficiency is not only due to the use of many segments but also due to the dramatic increase in the number of monitor units (MUs).[29] The increase in the number of MUs leads to leakage and head scatter and can affect the accuracy of treatment delivery.[19] More importantly, the increased exposure from complex IMRT plans may also increase the frequency of radiation-induced secondary malignancies. It has been recently reported that the transition from 3D conformal radiation therapy to IMRT resulted in a larger volume of normal tissue exposed to a low dose of radiation, which was estimated to increase the incidence of secondary cancers at 10 years from 1 to 1·75%.[30]

In our study, we have observed that the most of the segments were more than 100 in number, Figure 6, and attempts may be made to reduce the control points to reduce the MU for patient delivery.

https://doi.org/10.1017/S1460396921000017 Published online by Cambridge University Press

Table 4. Comparison of measured dose and calculated dose between I'MatriXX and TPS

Sr. no.	Field details	MU delivered at IMATRIX	Measured dose at IMATRIX	Calculated dose in TPS	Percentage difference
1	**AP**	234·165	27·32	28·571	−4·579
2	**LAO**	179·953	29·54	30·714	−3·974
3	**LPO**	223·625	27·54	28·571	−3·744
4	**RL**	119·902	29·21	28·571	2·188
5	**RAO**	109·836	41·55	40	3·73
6	**LPO**	165·148	42·54	40	5·971
7	**AP**	112·832	41·33	40	3·218
8	**LAO**	160·558	41·11	40	2·7
9	**RAO**	109·836	43·21	40	7·429
10	**AP**	201·688	23·45	22·222	5·237
11	**LAO**	177·882	22·14	22·222	−0·37
12	**LL**	208·978	23·54	22·222	5·599
13	**PA**	170·099	22·31	22·143	0·749
14	**PA**	153·426	23·11	22·222	3·842
15	**RPO**	179·962	23·33	22·222	4·749
16	**RAO**	160·68	23·45	22·222	5·237
17	**RPO1**	195·138	23·22	22·222	4·298
18	**LPO**	132·35	30·24	28·571	5·519
19	**LL**	151·47	29·24	28·571	2·288
20	**LAO**	157·807	29·21	28·571	2·188
21	**AP**	175·943	29·12	28·571	1·885
22	**RAO**	143·944	26·45	28·571	−8·019
23	**LPO**	189·658	30·12	28·571	5·143
24	**RPO**	154·049	29·15	28·571	1·986
25	**AP**	145·771	41·55	40	3·73
26	**LAO**	133·056	41·65	40	3·962
27	**AP**	226·925	32·66	31·429	3·769
28	**LAO**	263·999	32·54	31·429	3·414
29	**RL**	105·768	33·45	32·143	3·907
30	**AP**	220·147	31·55	30·429	3·553

Table 5. Statistical significance

	Number of fields	Mean percentage of deviation	Statistical significance
MU comparison between TPS and analytical method	30	1·03	<0·005
Comparison of measured dose and calculated dose between I'matrix and TPS	30	2·52	<0·005

The average numbers of control points were 151·43 ± 43. This indicates that the control points were in a significant number for every field. For 30 clinical cases and using formula 1, the mean MU per segment was 1·13 ± 0·214. Through this, it is understood that the minimum MU per segment will not be less than unity and hence the number of segments will lead to more number of MU for any IMRT delivery.

Some studies have been published in the domain of control points/segments. Some special algorithms reduce the total number of segments, while others minimise the total required MU.[31–35]

https://doi.org/10.1017/S1460396921000017 Published online by Cambridge University Press

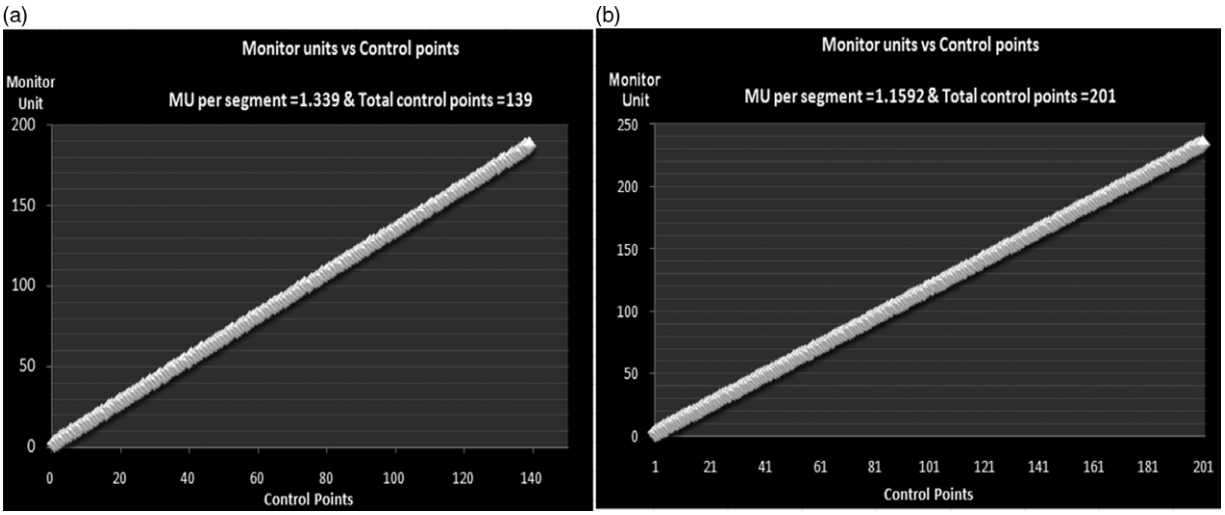

Figure 4: Relationship between the control point and monitor unit. (**a**) Relationship between CP and MU for MU/segment 1·339 and total control points 139. (**b**) Relationship between CP and MU for MU/segment 1·159 and total control points 201.

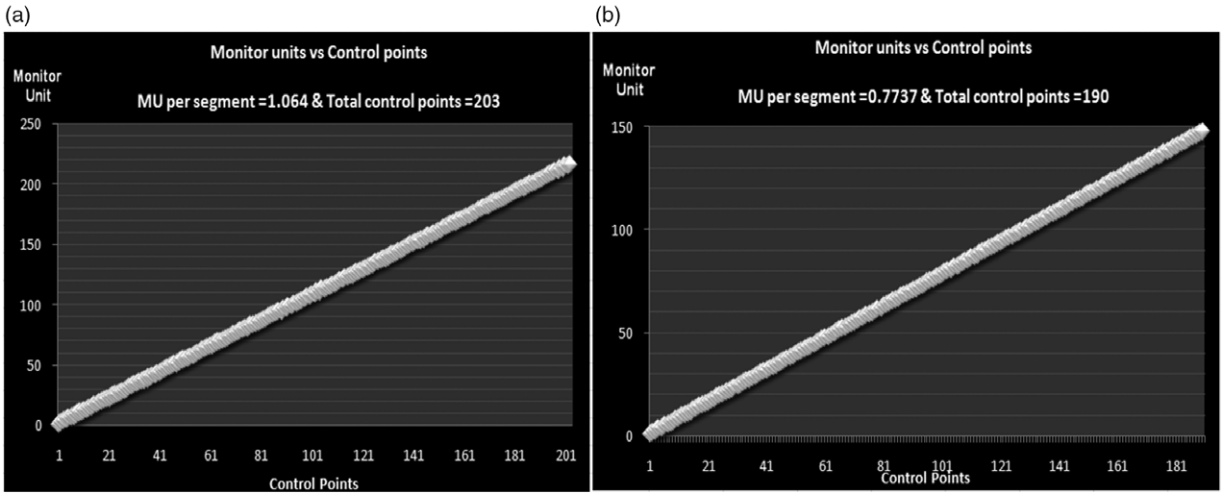

Figure 5. Relationship between the control point and monitor unit. (**a**) Relationship between CP and MU for MU/segment 1·064 and total control points 203. (**b**) Relationship between CP and MU for MU/segment 0·773 and total control points 190.

Other researchers have proposed the use of smoothing filters to eliminate unnecessary noise inside the intensity profiles, either during optimisation or before leaf sequencing.[35–37]

To simplify IMRT plans while improving delivery and radiation efficiency, many researchers have been working on increasing the efficiency of leaf sequencers.[34,38,39] Some leaf sequencers minimise the total number of segments, while others minimise the total required MUs.[36,40] With most commercial planning systems, options for controlling the complexity of an IMRT plan are often limited to choosing coarse intensity levels during conversion, selecting a leaf sequencer that can provide an optimal delivery efficiency for the specific delivery method (e.g., sliding window or step and shoot) or utilising smoothing filters.[41–43] However, the effectiveness of these methods in controlling the complexity of an IMRT plan is limited, often resulting in significant deteriorations in plan quality.

Conclusion

The control points are a potential parameter in the conventional IMRT delivery. Through this study, we have addressed the indirect method to estimate the monitor units delivered per segment with the TPS MU input. The average number of segments per IMRT treatment delivery and average MU per field were also estimated with the limits of 30 number of fields. The extension of this study can be performed as the methods to reduce the number of segments to achieve the same results without disturbing the plan quality in Eclipse TPS. Also, an analytical method can be found to estimate the MU per segment to be an independent method of MU calculation.

References

1. Jabbari K, Amouheidari A, Babazadeh S. The Quality Control of Intensity Modulated Radiation Therapy (IMRT) for ONCOR Siemens Linear Accelerators Using Film Dosimetry. y. Iran J Med Phys 2012; 9 (2):111–125.
2. Ma C M, Mok E, Kapur A et al. Clinical implementation of a Monte Carlo treatment planning system. Med Phys 1999; 26 (10): 2133–2143.
3. Al-Rahbi Z S, Al Mandhari Z, Ravichandran R, et al. Dosimetric comparison of intensity modulated radiotherapy isocentric field plans and field in field (FIF) forward plans in the treatment of breast cancer. J Med Phys 2013; 38 (1): 22–29.

https://doi.org/10.1017/S1460396921000017 Published online by Cambridge University Press

4. Khosla D, Patel F D, Oinam A S, Tomar P, Sharma S C. Dosimetric comparison of vaginal vault ovoid brachytherapy versus intensity-modulated radiation therapy plans in postoperative patients of cervical carcinoma following whole pelvic radiotherapy. J Cancer Res Ther 2014; 10 (1): 153–158.
5. Khan M I, Jiang R, Kiciak A, Ur Rehman J, Afzal M, Chow J C. Dosimetric and radiobiological characterizations of prostate intensity-modulated radiotherapy and volumetric-modulated arc therapy: a single-institution review of ninety cases. J Med Phys 2016; 41 (3): 162–168.
6. Wu V W C, Leung K Y. A Review on the Assessment of Radiation Induced Salivary Gland Damage After Radiotherapy. Front Oncol 2019; 9: 1090.
7. Boero I J, Paravati A J, Xu B et al. Importance of Radiation Oncologist Experience Among Patients With Head-and-Neck Cancer Treated With Intensity-Modulated Radiation Therapy. J Clin Oncol 2016; 34 (7): 684–690.
8. Convery D J, Rosenbloom L. The generation of intensity-modulated fields for conformal radiotherapy by dynamic collimation. Phys Med Biol 1991; 37: 1359–1374.
9. Chui C S, LoSasso T, Spirou S. Dose calculation for photon beams with intensity modulation generated by dynamic jaw or multileaf collimations. Med Phys 1994; 21 (8): 1237–1244.
10. Chang S X, Cullip T J, Deschesne K M. Intensity modulation delivery techniques: "step & amp; shoot" MLC auto-sequence versus the use of a modulator. Med Phys 2000; 27: 948–959.
11. Xia P, Verhey L J. Multileaf collimator leaf sequencing algorithm for intensity modulated beams with multiple static segments. Med Phys 1998; 25 (8): 1424–1434.
12. Galvin J M, Chen X G, Smith R M. Combining multileaf fields to modulate fluence distributions. Int J Radiat Oncol Biol Phys 1993; 27 (3): 697–705.
13. Chui C S, Spirou S, LoSasso T. Testing of dynamic multileaf collimation. Med Phys 1996; 23 (5): 635–641.
14. Otto K. Volumetric modulated arc therapy: IMRT in a single gantry arc. Med Phys 2008; 35 (1): 310–317.
15. Yu C X. Intensity-modulated arc therapy with dynamic multileaf collimation: an alternative to tomotherapy. Phys Med Biol 1995; 40 (9): 1435–1449.
16. LoSasso T, Chui C S, Ling C C. Physical and dosimetric aspects of a multileaf collimation system used in the dynamic mode for implementing intensity modulated radiotherapy. Med Phys 1998; 25 (10): 1919–1927.
17. Van Esch A, Huyskens D P, Behrens C F et al. Implementing Rapid Arc into clinical routine: a comprehensive program from machine QA to TPS validation and patient QA. Med Phys 2011; 38 (9): 5146–5166.
18. Ling C C, Burman C, Chui C S et al. Conformal radiation treatment of prostate cancer using inversely-planned intensity-modulated photon beams produced with dynamic multileaf collimation. Int J Radiat Oncol Biol Phys 1996; 35 (4): 721–730.
19. Mohan R, Arnfield M, Tong S, Wu Q, Siebers J. The impact of fluctuations in intensity patterns on the number of monitor units and the quality and accuracy of intensity modulated radiotherapy. Med Phys 2000; 27 (6): 1226–1237.
20. Tsai J S, Wazer D E, Ling M N, Wu J K et al. Dosimetric verification of the dynamic intensity-modulated radiation therapy of 92 patients. Int J Radiat Oncol Biol Phys 1998; 40 (5): 1213–1230.
21. Chen Z, Xing L, Nath R. Independent monitor unit calculation for intensity modulated radiotherapy using the MIMiC multileaf collimator. Med Phys 2002; 29 (9): 2041–2051.
22. Georg D, Garibaldi C, Dutreix A, Output ratios in a mini phantom for asymmetric fields shaped by a multileaf collimator. Phys Med Biol 1997; 42 (11); 2305–2317.
23. Xing L, Chen Y, Luxton G, Li J G, Boyer A L. Monitor unit calculation for an intensity modulated photon field by a simple scatter-summation algorithm. Phys Med Biol 2000; 45 (3): N1–N7.
24. Williams P C. IMRT: delivery techniques and quality assurance. Br J Radiol 2003;76 (911): 766–776.
25. Wang X, Spirou S, LoSasso T, Stein J, Chui C S, Mohan B. Dosimetric verification of intensity-modulated fields. Med Phys 1996; 23 (3): 317–327.
26. Xing L, Curran B, Hill R, Holmes T, Ma L, Forster K M, Boyer A L. Dosimetric verification of a commercial inverse treatment planning system. Phys Med Biol 1999; 44 (2): 463–478.
27. Ludlum E, Akazawa C, Xia P: IMRT plans can be simplified using one step optimization. Med Phys 2006; 33 (6): 2111.
28. IMRT, IGRT, SBRT- Advances in the Treatment Planning and delivery of Radiotherapy, 2nd Edition.
29. Galvin J M, Ezzell G, Eisbrauch A, et al. American Society for Therapeutic Radiology and Oncology; American Association of Physicists in Medicine. Implementing IMRT in clinical practice: a joint document of the American Society for Therapeutic Radiology and Oncology and the American Association of Physicists in Medicine. Int J Radiat Oncol Biol Phys 2004; 58 (5): 1616–1634.
30. Hall E J, Wuu C S. Radiation-induced second cancers: the impact of 3D-CRT and IMRT. Int J Radiat Oncol Biol Phys 2003; 56 (1): 83–88.
31. Hansen E K, Bucci M K, Quivey J M, Weinberg V, Xia P. Repeat CT imaging and replanning during the course of IMRT for head-and-neck cancer. Int J Radiat Oncol Biol Phys 2006; 64 (2): 355–362.
32. Yan D, Vicini F, Wong J, Martinez A: adaptive radiation therapy. Phys Med Biol 1997; 42: 123–132.
33. Ludlum E, Xia P. Comparison of IMRT planning with two-step and one-step optimization: a way to simplify IMRT. Phys Med Biol 2008; 53 (3): 807–821.
34. Kamath S, Sahni S, Li J, Palta J, Ranka S. Leaf sequencing algorithms for segmented multileaf collimation. Phys Med Biol 2003; 48 (3): 307–324.
35. Siebers J V, Lauterbach M, Keall P J, Mohan R. Incorporating multi-leaf collimator leaf sequencing into iterative IMRT optimization. Med Phys 2002; 29 (6): 952–959.
36. Sun X, Xia P. A new smoothing procedure to reduce delivery segments for static MLC-based IMRT planning. Med Phys 2004; 31 (5): 1158–1165.
37. Crooks S M, McAven L F, Robinson D F, Xing L. Minimizing delivery time and monitor units in static IMRT by leaf-sequencing. Phys Med Biol 2002; 47 (17): 3105–3116.
38. Bednarz G, Michalski D, Houser C, Huq M S, Xiao Y, Anne P R, Galvin J M. The use of mixed-integer programming for inverse treatment planning with pre-defined field segments. Phys Med Biol 2002; 47 (13): 2235–2245.
39. Spirou S V, Fournier-Bidoz N, Yang J, Chui C S, Ling C C. Smoothing intensity-modulated beam profiles to improve the efficiency of delivery. Med Phys 2001; 28 (10): 2105–2112.
40. Coselmon M M, Moran J M, Radawski J D, Fraass B A. Improving IMRT delivery efficiency using intensity limits during inverse planning. Med Phys 2005; 32 (5): 1234–1245.
41. Keller-Reichenbecher M A, Bortfeld T, Levegrün S, Stein J, Preiser K, Schlegel W. Intensity modulation with the "step and shoot" technique using a commercial MLC: a planning study. Multileaf collimator. Int J Radiat Oncol Biol Phys 1999; 45 (5): 1315–1324.
42. Seco J, Evans P M, Webb S. An optimization algorithm that incorporates IMRT delivery constraints Phys Med Biol 2002; 47: 899–915.
43. IMRT, IGRT, SBRT- Advances in the Treatment Planning and delivery of Radiotherapy, 2nd Edition.

https://doi.org/10.1017/S1460396921000017 Published online by Cambridge University Press